

# The Higgs masses and explicit CP violation in the gluino-axion model

Müge Boz

Physics Department, Hacettepe University, 06532, Beytepe, Ankara

## Abstract

In this work, we address the phenomenological consequences of explicit CP violation on direct Higgs-boson searches at high energy colliders. Having a restricted parameter space, we concentrate on the recently proposed gluino-axion model, and investigate the CP violation capability of the model subject to the recent experimental data. It is shown that the Higgs masses as well as their CP compositions are quite sensitive to the supersymmetric CP phases. The lightest Higgs is found to be nearly CP even to a good approximation whilst the remaining two heavy scalars do not have definite CP parities.

# 1 Introduction

Presently, the phenomenon of CP non-conservation is one of the key problems from both theoretical and experimental points of views. The observed CP violation in neutral kaon system [1] as well as the electric dipole moment (EDM) of the neutron [2] severely constrain the sources and strength of CP violation in the underlying model. In the standard model (SM) both strong and electroweak interactions violate the CP invariance. It is a well-known fact that the  $\theta$  vacuum [3] violates the CP invariance, and results in a neutron EDM exceeding the present bounds by nine orders of magnitude [4]. This is the source of the strong CP problem – a CP hierarchy and naturalness problem.

In the supersymmetric (SUSY) extensions of the standard electroweak theory (SM) this hierarchy problem still persists. Moreover, there appear novel sources of CP violation coming from the soft supersymmetry breaking mass terms. Though the phases of the soft terms have been shown to relax to CP-conserving points in the minimal model (MSSM) [5], this is not necessarily true in the non-minimal model (NMSSM) [6] containing a singlet. These soft terms contribute to known CP-violating observables [7] (EDM's and neutral meson mixings); however, they also induce CP violation in the Higgs sector[8, 9, 10, 11].

In addition to these CP hierarchy problems, in minimal SUSY model there is another hierarchy problem concerning the Higgsino Dirac mass parameter ( $\mu$ ), that is, this mass parameter follows from the superpotential of the model and there is no telling of at what scale (ranging from  $M_W$  to  $M_{Pl}$ ) it is stabilized.

In a recently proposed model so called as gluino-axion[12, 13] the two hierarchy problems, i.e, the strong CP problem and the  $\mu$  problem are solved in the context of supersymmetry with a new kind of axion [14, 15] which couples to the gluino rather than to quarks. In this model the invariance of the supersymmetric Lagrangian and all supersymmetry breaking terms under  $U(1)_R$  is guaranteed by promoting the ordinary  $\mu$  parameter to a composite operator involving the gauge singlet  $\hat{S}$  with unit  $R$  charge. When the scalar component of the singlet develops vacuum expectation value (VEV) around the Peccei–Quinn scale  $\sim 10^{11} \text{ GeV}$  an effective  $\mu$  parameter  $\mu \sim \text{a TeV}$  is induced. Besides, the low energy theory is identical to minimal SUSY model

with all sources of soft supersymmetric phases. Due to all these abilities of the model of Ref. 12 in solving the hierarchy problems, in the analysis below we will adopt its parameter space.

In this work, we address the consequences of explicit CP violation on the the radiatively corrected Higgs masses and mixings in the framework of the gluino-axion model. It will be seen that the supersymmetric phases significantly affect the Higgs masses and mixings thereby giving new regions in the parameter space (otherwise excluded) meeting the recent LEP constraints [16]. As a result of the standard model Higgs boson searches at LEP, the lower bound on the lightest Higgs mass is 115 GeV (and correspondingly  $\tan\beta \gtrsim 3.5$ )[16]. On the other hand, theoretically the lightest Higgs boson mass can not exceed 130 GeV for large  $\tan\beta$  [17]. Therefore, from the searches at LEP2, the lower limit on mass of the SM Higgs boson excludes the substantial part of the MSSM parameter space particularly at small  $\tan\beta$  ( $\tan\beta \lesssim 3.5$ )[16].

It is a well-known fact that, CP is conserved in the Higgs sector of the minimal supersymmetric model (MSSM) at the tree level. On the other hand, the radiative corrections to the masses of the Higgs bosons, dominated by top-quark and top-squark loops, have been found to modify significantly the tree level bound [18, 19]. The CP conserving Higgs sector has been analyzed by several authors and the radiative corrections which make very important contributions to the Higgs masses have been computed by using different approximations such as diagrammatic [18, 20] and effective potential methods [19]. More complete treatment of these results include the complete one-loop on-shell renormalization [21], the renormalization group (RG) improvement for resumming the leading logarithms[22], the iteration of the RG equations to two-loops with the use of the effective potential techniques[23] and the two loop on-shell renormalization [17, 24].

On the other hand, as is indicated in Ref. 9 that the explicit CP violation in the matrices of third generation squarks can induce CP violation through loop corrections. In the recent literature, the radiatively induced CP violation effects has been studied without [9, 10, 11, 25] or with [26, 27] RG improvement. In between these works, the diagrammatic computation of the scalar-pseudoscalar transitions was the the scope of Ref. 9, where the implications of the presence of CP phases in the soft SUSY breaking sector

allowing to the mixing of CP even and CP odd states were discussed. More recently, the mass matrix of the neutral Higgs bosons of the MSSM has been calculated with the effective potential method in Refs. 10 and 11 from different perspectives. The detailed analysis of underlying dynamics under study is performed in case of the small splittings between squark mass eigenstates in Ref. 10; whereas bottom-sbottom contributions are not taken into account in Ref. 11. Additional contributions from the chargino, W and the charged Higgs exchange loops were computed in Ref. 25. In Ref. 26, one-loop corrections to the mass matrix of the neutral Higgs bosons in the MSSM were calculated by using the effective potential method for an arbitrary splitting between squark masses, including the electroweak and gauge couplings and the leading two loop corrections. Although, the earlier works [10, 11] on the Higgs spectrum were based on some approximations, the results are in agreement with the ones presented Ref. 26 in the appropriate limit. More complete treatment of the effective Higgs potential in the MSSM including the two-loop leading logarithms induced by top-bottom Yukawa couplings as well as those associated with QCD corrections by means of RG methods were performed in Ref. 27 in which the leading logarithms generated by one-loop gaugino and higgsino quantum effects are also taken into consideration.

We would like to point out that, it is the main purpose of this work to investigate the CP violation capability of the gluino-axion model. Therefore, we limit our analysis to the effective potential with no RG improvement. This accuracy has proven sufficient in obtaining the observable effects of explicit CP violation on the Higgs masses and mixings [11]. In the following, we compute the radiatively corrected Higgs masses and mixings, taking into account the CP violation effects. We will base our calculations to those of Ref. 11, by modifying the parameters appropriately in connection with the gluino- axion model. The main difference with the previous work [8, 11] springs from the fact that the parameters chosen are specific to the gluino- axion model, namely all the soft mass parameters in this theory are fixed in terms of the  $\mu$  parameter.

The organization of this work is as follows: In Sec. 2, starting from the Higgs sector structure of the gluino-axion model, we compute the  $(3 \times 3)$  dimensional mass matrix of the Higgs scalars in which all the elements are expressed in terms of the parameters of the model under concern. In Sec.

3, we make the numerical analysis for evaluating the masses of the Higgs bosons and analyzing the relative strengths of CP-violating and CP-conserving mixings. In Sec. 4, we conclude the work.

## 2 Higgs Sector in the Gluino-Axion Model

In this section, our starting point will be the description of the basic low-energy structure of the gluino-axion model which contains the sources of explicit CP violation. The gluino-axion model, is defined by the superpotential

$$\widehat{W} = \mu(\widehat{S}) \widehat{H}_u \cdot \widehat{H}_d + m_s^2 \mu(\widehat{S}) + h_u \widehat{Q} \cdot \widehat{H}_u \widehat{u}_c + h_d \widehat{Q} \cdot \widehat{H}_d \widehat{d}_c + h_e \widehat{L} \cdot \widehat{H}_d \widehat{e}_c \quad (1)$$

where  $\widehat{Q}$ ,  $\widehat{u}_c$ ,  $\widehat{d}_c$ ,  $\widehat{L}$ ,  $\widehat{e}_c$  are the quark, lepton and  $\widehat{H}_u$ ,  $\widehat{H}_d$  are the Higgs superfields respectively. The model, replaces  $\mu$  with the composite operator containing the singlet composite superfield  $\widehat{S}$  of  $R=+1$  so that the resulting supersymmetric Lagrangian and all supersymmetry breaking terms are invariant under  $U(1)_R$  [12]. The pure singlet contribution  $m_s^2 \mu(\widehat{S})$  in  $\widehat{W}$  is allowed by the symmetries of the model.

The soft terms of the low energy Lagrangian in the gluino-axion model are identical to those in the general MSSM <sup>1</sup>

$$\begin{aligned} \mathcal{L}_{MSSM}^{soft} = & \tilde{Q}^\dagger M_Q^2 \tilde{Q} + \tilde{u}^c \tilde{u}^c + \tilde{d}^c \tilde{d}^c + \tilde{L}^\dagger M_L^2 \tilde{L} + \tilde{e}^c \tilde{e}^c \\ & + \{ A_u \tilde{Q} \cdot H_u \tilde{u}^c + A_d \tilde{Q} \cdot H_d \tilde{d}^c + A_e \tilde{L} \cdot H_d \tilde{e}^c \} + h.c. \\ & + M_{H_u}^2 |H_u|^2 + M_{H_d}^2 |H_d|^2 + (\mu B H_u \cdot H_d + h.c.) \\ & + \{ M_3 \tilde{\lambda}_3^a \tilde{\lambda}_3^a + M_2 \tilde{\lambda}_2^i \tilde{\lambda}_2^i + M_1 \tilde{\lambda}_1 \tilde{\lambda}_1 + h.c. \}, \end{aligned} \quad (2)$$

except for the fact that the soft masses are all expressed in terms of the  $\mu$  parameter through appropriate flavour matrices. The flavour matrices form the sources of CP violation and intergenerational mixings in the squark sector. The phases of the trilinear couplings ( $A_{u,d,e}$ ), the gaugino masses ( $M_{3,2,1}$ ), and the effective  $\mu$ -parameter

$$\mu \equiv v_s^2 / M_{Pl} \times e^{-i\theta_{QCD}/3} \sim \text{a TeV} \times e^{-i\theta_{QCD}/3} \quad (3)$$

---

<sup>1</sup>Here and in what follows we will neglect the effects of axion, axino, and saxino as their couplings are severely suppressed [12].

are the only phases which can generate CP violation observables. In this formula for the  $\mu$  parameter  $v_s \sim 10^{11}$  GeV is the Peccei–Quinn scale, and  $\theta_{QCD}$  is the effective QCD vacuum angle. One notes that the vacuum expectation value of the singlet serves for two important purposes for the model under concern: Its magnitude determines the scale of supersymmetry breaking and its phase solves the strong CP–problem.

In the following, we shall calculate the one-loop corrections to the Higgs masses and mixings. In doing this, we will modify the parameters in connection with the gluino-axion model. As in the CP-conserving case [18, 19], among the particles contributing to the one-loop radiative corrections, the dominant ones come from the top quark and top squark loops provided that  $\tan \beta \lesssim 50$  (in which case the bottom Yukawa coupling is too small to give significant contributions). The Yukawa interactions due to scalar-bottom quarks can be significant only for very large  $\tan \beta$  values. On the other hand, the contributions of gauginos and Higgsinos are already negligible since they couple via weak coupling. In our analysis we restrict ourselves for the case  $\tan \beta \lesssim 50$ , so that the dominant terms will be given by the top quark and top squark loops, to a good approximation. Therefore, we will not need the full flavour structures in Ref. 12, instead we will need to specify only the top squark sector:

(i) The top squark soft masses:

$$M_Q^2 = k_Q^2 |\mu|^2, \quad M_{\tilde{u}}^2 = k_u^2 |\mu|^2, \quad M_{\tilde{d}}^2 = k_d^2 |\mu|^2 \quad (4)$$

where  $k_{Q,u,d}$  are real parameters.

(ii) The top squark trilinear coupling

$$A_t = \mu^* k_t, \quad (5)$$

where  $k_t$  is a complex parameter.

Other than these soft masses, it is necessary to know the tree level Higgs soft masses

$$M_{H_u}^2 = y_u |\mu^2|, \quad M_{H_d}^2 = y_d |\mu^2|, \quad \mu B = |\mu|^2 \left( \frac{8m_s^2}{v_s^2} + k_\mu \right), \quad (6)$$

where  $m_s^2 \sim v_s^2$  is a natural choice as discussed in Ref. [12]. Here  $y_u$  and  $y_d$  are real parameters, and  $k_\mu$  is a complex parameter determining the phase of the  $B$  parameter. As was analyzed in Ref. 11 in detail this phase can be

identified with the relative phase of the Higgs doublets; hence, there is no CP violation in Higgs sector of (2) at tree level.

After electroweak breaking the Higgs doublets in (2) can be expanded as

$$\begin{aligned} H_d &= \begin{pmatrix} H_d^0 \\ H_d^- \end{pmatrix} = \frac{1}{\sqrt{2}} \begin{pmatrix} v_d + \phi_1 + i\varphi_1 \\ H_d^- \end{pmatrix}, \\ H_u &= \begin{pmatrix} H_u^+ \\ H_u^0 \end{pmatrix} = \frac{e^{i\theta}}{\sqrt{2}} \begin{pmatrix} H_u^+ \\ v_u + \phi_2 + i\varphi_2 \end{pmatrix}. \end{aligned} \quad (7)$$

where  $\tan \beta \equiv v_u/v_d$  as usual, and the angle parameter  $\theta$  is the misalignment between the two Higgs doublets. As in Ref. 11 the angle  $\theta$  gets embedded into the total CP violation angle  $\text{Arg}[\mu A_t]$ , and we will not elaborate radiative corrections to it [28].

As usual, we calculate the Higgs masses and their mixings up to one loop accuracy via

$$M^2 = \left( \frac{\partial^2 V}{\partial \chi_i \partial \chi_j} \right)_0, \text{ where } \chi_i \in \mathcal{B} = \{\phi_1, \phi_2, \varphi_1, \varphi_2\}. \quad (8)$$

where  $V \equiv V_0 + V_{1-loop}$  is the radiatively corrected Higgs potential [11]. As mentioned before, we take into account only top quark and top squark loop corrections, which are the dominant ones as long as  $\tan \beta \lesssim 50$ . The radiative corrections depend on the stop mass-squared eigenvalues  $m_{\tilde{t}_{1,2}}^2$ ,

$$m_{\tilde{t}_{1,2}}^2 = \frac{1}{2} \left( (k_u^2 + k_Q^2) |\mu|^2 + 2m_t^2 \mp \Delta_t^2 \right), \quad (9)$$

whose splitting

$$\Delta_t^2 = |\mu| \sqrt{(k_u^2 - k_Q^2)^2 |\mu|^2 + 4m_t^2 (|k_t|^2 + \cot^2 \beta - 2|k_t| \cot \beta \cos \varphi_{kt})}. \quad (10)$$

will play a key rôle in analyzing the results as it depends explicitly on the total CP violation angle

$$\varphi_{kt} = \text{Arg}[\mu A_t] = \text{Arg}[k_t] \quad (11)$$

where  $k_t$  has been defined in (5). One here notices that  $\Delta_t^2$  increases as  $\varphi_{kt}$  changes from 0 to  $\pi$ . This particularly means that the strength of the radiative corrections are modified as  $\varphi_{kt}$  ranges from one CP-conserving point to the next.

We express the  $(3 \times 3)$  dimensional Higgs mass-squared matrix

$$M^2 = \begin{pmatrix} M_{11} + \Delta M_{11} & M_{12} + \Delta M_{12} & \Delta M_{13} \\ M_{12} + \Delta M_{12} & M_{22} + \Delta M_{22} & \Delta M_{23} \\ \Delta M_{13} & \Delta M_{23} & M_{33} + \Delta M_{33} \end{pmatrix}, \quad (12)$$

in the basis  $\mathcal{B} = \{\phi_1, \phi_2, \sin \beta \varphi_1 + \cos \beta \varphi_2\}$  using (7). The elements of the mass matrix read as below:

$$\begin{aligned} M_{11} &= M_Z^2 \cos^2 \beta + \tilde{M}_A^2 \sin^2 \beta, \\ M_{12} &= -(M_Z^2 + \tilde{M}_A^2) \sin \beta \cos \beta, \\ M_{22} &= M_Z^2 \sin^2 \beta + \tilde{M}_A^2 \cos^2 \beta, \\ M_{33} &= \tilde{M}_A^2, \end{aligned} \quad (13)$$

where the radiative corrections are generically denoted by  $\Delta M_{ij}$ . In the case of CP-conserving limit in which CP-even and CP-odd sectors in (12) decouple,  $\tilde{M}_A^2$  becomes the radiatively corrected pseudoscalar mass and  $\Delta M_{11,12,22}$  become the usual one-loop corrections to the CP even scalar mass-squared matrix [18, 19]. On the other hand,  $\Delta M_{13}$  and  $\Delta M_{23}$  are genuinely generated by the SUSY CP-violation effects. We define

$$\begin{aligned} \mathcal{R}_{kt} &= |k_t| \cos \varphi_{kt} - \cot \beta, \\ \mathcal{L}_{kt} &= |k_t| - \cot \beta \cos \varphi_{kt}, \\ \mathcal{C}_{kt} &= (|k_t| - \cot \beta) \sin^2 \varphi_{kt}. \end{aligned} \quad (14)$$

These radiative correction terms have the following expressions:

$$\Delta M_{11} = -2\beta_{ht} |\mu|^4 m_t^2 \frac{\mathcal{R}_{kt}^2}{\Delta_{\tilde{t}}^4} g(m_{\tilde{t}_1}^2, m_{\tilde{t}_2}^2), \quad (15)$$

$$\begin{aligned} \Delta M_{12} &= -2\beta_{ht} m_t^2 |\mu|^2 \left[ \frac{\mathcal{R}_{kt}}{\Delta_{\tilde{t}}^2} \log \frac{m_{\tilde{t}_2}^2}{m_{\tilde{t}_1}^2} \right. \\ &\quad \left. - |\mu|^2 |k_t| \frac{\mathcal{R}_{kt}^2 + |k_t| \mathcal{C}_{kt}}{\Delta_{\tilde{t}}^4} g(m_{\tilde{t}_1}^2, m_{\tilde{t}_2}^2) \right], \end{aligned} \quad (16)$$

$$\begin{aligned} \Delta M_{22} &= 2\beta_{ht} m_t^2 \left[ \log \frac{m_{\tilde{t}_2}^2 m_{\tilde{t}_1}^2}{m_t^4} + 2|k_t| |\mu|^2 \frac{\mathcal{L}_{kt}}{\Delta_{\tilde{t}}^2} \log \frac{m_{\tilde{t}_2}^2}{m_{\tilde{t}_1}^2} \right. \\ &\quad \left. - |k_t|^2 |\mu|^4 \frac{\mathcal{L}_{kt}^2}{\Delta_{\tilde{t}}^4} g(m_{\tilde{t}_1}^2, m_{\tilde{t}_2}^2) \right], \end{aligned} \quad (17)$$

$$\Delta M_{13} = -2\beta_{h_t} m_t^2 |\mu|^4 |k_t| \frac{\sin \varphi_{kt}}{\sin \beta} \frac{\mathcal{R}_{kt}}{\Delta_t^4} g(m_{\tilde{t}_1}^2, m_{\tilde{t}_2}^2) , \quad (18)$$

$$\begin{aligned} \Delta M_{23} &= -2\beta_{h_t} m_t^2 \frac{|\mu|^4 |k_t|^2 \sin \varphi_{kt}}{\Delta_t^4} \\ &\times [\mathcal{L}_{kt} - \frac{1}{|k_t| |\mu|^2 g(m_{\tilde{t}_1}^2, m_{\tilde{t}_2}^2)} \Delta_t^2 \log \frac{m_{\tilde{t}_2}^2}{m_{\tilde{t}_1}^2}] , \end{aligned} \quad (19)$$

$$\Delta M_{33} = -2\beta_{h_t} m_t^2 \frac{\sin \varphi_{kt}^2}{\sin \beta^2} \frac{|\mu|^4 |k_t|^2}{\Delta_t^4} g(m_{\tilde{t}_1}^2, m_{\tilde{t}_2}^2) , \quad (20)$$

where  $\beta_{h_t} = 3h_t^2/16\pi^2$ , and the function  $g(x, y)$  is defined by

$$g(m_{\tilde{t}_1}^2, m_{\tilde{t}_2}^2) = -2 + \frac{m_{\tilde{t}_2}^2 + m_{\tilde{t}_1}^2}{m_{\tilde{t}_2}^2 - m_{\tilde{t}_1}^2} \log \frac{m_{\tilde{t}_2}^2}{m_{\tilde{t}_1}^2} . \quad (21)$$

We diagonalize the Higgs mass-squared matrix (12) by the similarity transformation

$$\mathcal{R}M^2\mathcal{R}^T = \text{diag}(m_{h_1}^2, m_{h_2}^2, m_{h_3}^2) , \quad (22)$$

where  $\mathcal{R}\mathcal{R}^T = 1$ . In the following, we define  $h_3$  to be the lightest of all three;  $h_2$  to be the one that corresponds to the heavy pseudoscalar Higgs boson and  $h_1$  to be the heavy CP-even scalar Higgs boson. One of the most important quantities in our analyses is the percentage CP composition of a given mass-eigenstate Higgs boson. The percentage CP compositions of the Higgs bosons in terms of the basis elements are defined by

$$\rho_i = 100 \times |\mathcal{R}_{1i}|^2; \quad i = 1, 2, 3. \quad (23)$$

where  $\rho_1$ ,  $\rho_2$  and  $\rho_3$  correspond respectively the  $\phi_1$ ,  $\phi_2$ ,  $\sin \beta \varphi_1 + \cos \beta \varphi_2$  components of the Higgs boson under concern.

In what follows, we will make the numerical analysis for evaluating the masses of the Higgs scalars and analyzing the relative strengths of their percentage CP compositions under the effects of SUSY CP phases. In doing this, we will first focus on the percentage CP compositions of the lightest Higgs boson ( $h_3$ ), especially its CP-odd composition ( $\rho_3$ ), which can offer new opportunities at colliders for observing the Higgs boson [8, 29]. We will

discuss the dependence of the CP odd compositions of  $h_3$  on the CP-breaking angle in reference to the previous theoretical [8, 11] as well as the recent experimental bounds [16]. Next, we will analyze the masses and the percentage CP compositions of the remaining two heavy scalars ( $h_1, h_2$ ) in the low and high  $\tan \beta$  regimes.

### 3 Numerical Analysis

Using the formulae in the last section, we will now analyze several quantities in a wide range of the parameter space. As a reflecting property of the model, all parameters are expressed in terms of the  $\mu$  parameter. Since the  $\mu$  parameter is already stabilized to the weak scale, as a consequence of the naturalness, all dimensionless quantities are expected to be  $\mathcal{O}(1)$ . Therefore, as a representative point in the parameter space we take

$$k_Q = k_u = |k_t| = 1 , \quad (24)$$

In our analysis,  $|\mu|$  changes from  $250 \text{ GeV}$  to  $1000 \text{ GeV}$  and  $M_A$  from  $|\mu|$  to  $5 |\mu|$  for each  $\mu$  value in the full  $\varphi_{kt}$  range. However, we would like to note that for the values of  $\mu \lesssim 450 \text{ GeV}$ , it is not possible to find regions in the parameter space satisfying the recent LEP constraints [16]. Moreover, we concentrate on the two specific values of  $\tan \beta$  namely  $\tan \beta = 4$  and  $\tan \beta = 30$  to analyze the behaviour of the Higgs masses and mixings in the small and large  $\tan \beta$  regimes in detail.

Fig. 1 illustrates the dependence of the lightest Higgs mass  $m_{h_3}$  on  $\varphi_{kt}$  for  $\tan \beta = 4$  (left panel) and  $\tan \beta = 30$  (right panel). One immediately observes that  $m_{h_3}$  increases with  $\varphi_{kt}$  for  $\tan \beta = 4$  (left panel), whereas it remains nearly constant for  $\tan \beta = 30$  (right panel) in the  $[0, \pi]$  interval. This saturation effect in the Higgs mass can be easily understood by observing that the radiative corrections depend strongly on the stop splitting  $\Delta_{\tilde{t}}^2$ . This quantity depends explicitly on  $\varphi_{kt}$  such that:

$$\frac{\Delta_{\tilde{t}}^2(\pi)}{\Delta_{\tilde{t}}^2(0)} \sim \sqrt{\frac{1 + \sin 2\beta}{1 - \sin 2\beta}} , \quad (25)$$

that is, the stop splitting  $\Delta_{\tilde{t}}^2$  increases with increasing  $\varphi_{kt}$ , as  $\varphi_{kt}$  changes from  $0$  to  $\pi$ . This particularly implies that the strength of the radiative

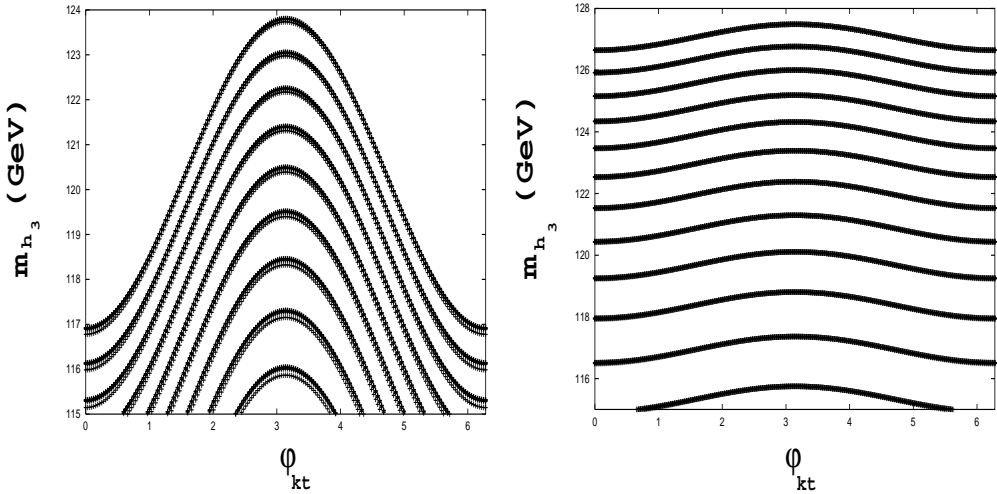


Figure 1: The mass ( $m_{h_3}$ ) of the lightest Higgs boson ( $h_3$ ), as a function of  $\varphi_{kt}$  for  $\tan \beta = 4$  (left panel) and  $\tan \beta = 30$  (right panel).

corrections modify as  $\varphi_{kt}$  changes from one CP-conserving point to the next. However, (25) decreases with increasing  $\tan \beta$ . Indeed, it approaches to unity in the large  $\tan \beta$  limit. Therefore, the radiative corrections to the lightest Higgs mass  $m_{h_3}$  which are sensitive to variations in  $\varphi_{kt}$  are suppressed in large  $\tan \beta$  regime. In the light of these observations, it is clear that the lightest Higgs mass  $m_{h_3}$  is much more flat for  $\tan \beta = 30$  (right panel) compared to that for  $\tan \beta = 4$  (left panel).

As the left panel of Fig. 1 suggests that, the  $\varphi_{kt}$  dependence of  $m_{h_3}$  around ( $\phi_{kt} = \pi$ ) differs from those at other CP-conserving points, in particular for the case of  $\tan \beta = 4$ . That is, the maximal value of the lightest Higgs mass  $m_{h_3}$  occurs at ( $\phi_{kt} = \pi$ ), and then, the radiative corrections reverse their sign as  $\varphi_{kt}$  changes from  $\pi$  to  $2\pi$  (see (9), (10)). Numerically, for  $\tan \beta = 4$ ,  $m_{h_3}(\phi_{kt} = \pi)$  is larger than  $m_h(\phi_{kt} = 0)$  by  $\sim 10$  GeV due to the enhancements in the radiative corrections as  $\varphi_{kt}$  ranges from 0 to  $\pi$ . In contrast to  $\tan \beta = 4$  case, the sensitivity of the lightest Higgs mass  $m_{h_3}$  on  $\varphi_{kt}$  is washed out in the large  $\tan \beta$  regime due to the reasons explained above (25).

It is known that the recent experimental data requires  $m_{h_3} \gtrsim 115$  GeV [16]. Imposing this constraint on  $m_{h_3}$ , the experimental bound on the lightest Higgs mass is satisfied for all the parameter space, for which  $\tan \beta = 4$  and  $\tan \beta = 30$ . The dependence of the Higgs mass on the CP violation angle

has also been noted in Ref. 8, for general minimal supersymmetric standart model with a limited range of the parameters.

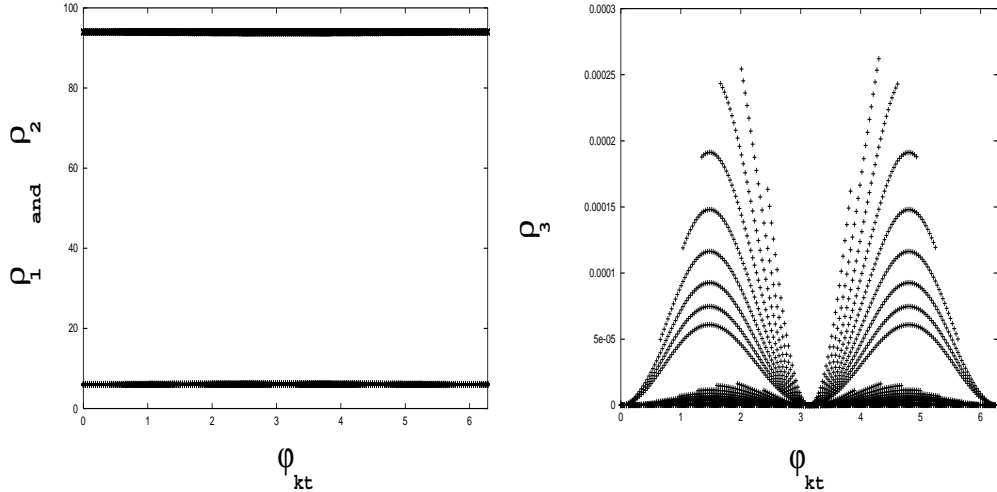


Figure 2: The percentage CP-even compositions of the lightest Higgs boson  $h_3$  (left panel) where the bottom and the top curves present  $\rho_1$  and  $\rho_2$ , respectively, and its percentage CP-odd composition  $\rho_3$  (right panel), as a function of  $\varphi_{kt}$  for  $\tan\beta=30$ .

In Fig. 2, we show the  $\varphi_{kt}$  dependence of the percentage CP-even,  $\rho_1-\rho_2$ , (left panel), and the percentage CP-odd  $\rho_3$  (right panel) compositions of the lightest Higgs boson ( $h_3$ ), for  $\tan\beta = 4$ . As is seen from the left panel Fig. 2,  $h_3$  has  $\approx 94\% \rho_2$  and  $\approx 6\% \rho_1$  compositions for  $\tan\beta = 4$ . On the other hand, the right panel of Fig. 2 suggests that its percentage CP-odd composition  $\rho_3$  is extremely small for small  $\tan\beta$  regime. Numerically, the maximum value of  $\rho_3$  is  $\approx 0.0003\%$  in the full range of  $\varphi_{kt}$  for  $\tan\beta = 4$  (right panel).

Depicted in Fig. 3 is the percentage composition CP-even,  $\rho_1-\rho_2$ , (left panel), and percentage CP-odd  $\rho_3$  (right panel) compositions of the lightest Higgs boson ( $h_3$ ), for  $\tan\beta = 30$ . One notes that  $\rho_2$  increases near to the  $\approx 99.9\%$ , while  $\rho_1$  remains below  $\approx 0.12\%$  for  $\tan\beta = 30$ . On the other hand, as is seen from the right panel of Fig. 3, the percentage CP-odd composition ( $\rho_3$ ) of the lightest Higgs boson ( $h_3$ ) is still very small. However, it increases relatively as compared to that for  $\tan\beta = 4$  (left panel), and reaches to a maximum value of  $\approx 0.0013\%$  for  $\tan\beta = 30$  in the entire range of  $\varphi_{kt}$ .

One notes that the CP-odd component of  $h_3$  never exceeds  $0.0013\%$  in the full  $\varphi_{kt}$  range, for all values of  $\tan\beta$  changing from 4 to 30. Compared to its

CP–even compositions, which form the remaining percentage, this CP–odd component is extremely small to cause observable effects. It may, however, be still important when the radiative corrections to gauge and Higgs boson vertices are included [8].

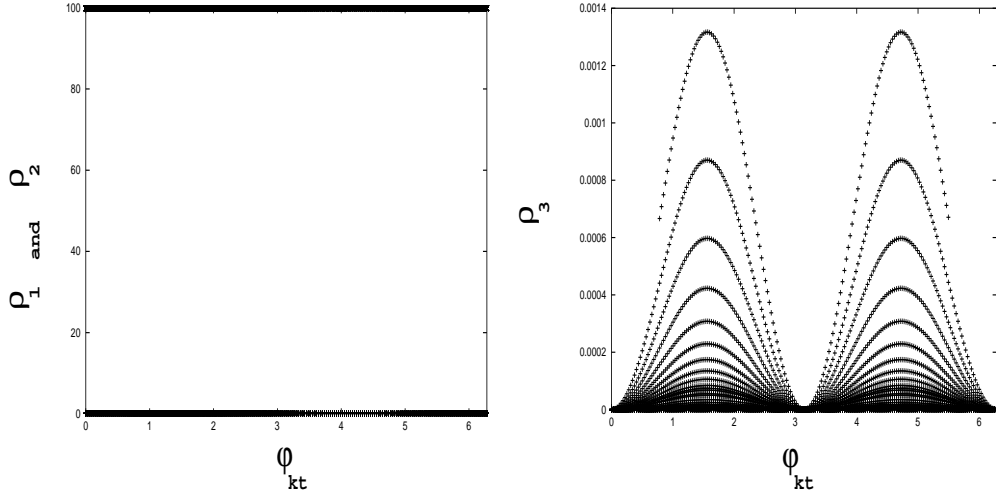


Figure 3: The percentage CP–even compositions of the lightest Higgs boson  $h_3$  (left panel) where the bottom and the top curves present  $\rho_1$  and  $\rho_2$ , respectively, and its percentage CP–odd composition  $\rho_3$  (right panel), as a function of  $\varphi_{kt}$  for  $\tan \beta=30$ .

Depicted Fig. 4 is the  $|\mu|$  dependence of  $\rho_3$  designating the CP–odd percentage composition of  $h_3$ , for  $\tan \beta = 4$ (left panel), and  $\tan \beta = 30$ (right panel), respectively. Both the left and right panels of Fig. 4 suggest that the CP–odd percentage composition of  $h_3$  ( $\rho_3$ ) decreases with  $|\mu|$ . It is also seen from the left panel of Fig. 4 that , the maximum value of  $\rho_3$  ( $\approx 0.00027\%$ ) occurs at  $|\mu| \approx 650 \text{ GeV}$ . For larger values of  $|\mu|$ ,  $\rho_3$  decreases gradually as the supersymmetric spectrum decouples. For smaller values of  $|\mu|$ , however, the parameter space is constrained by the existing LEP bound on the lightest Higgs mass [16]. That is, the CP–odd percentage composition of  $h_3$  ( $\rho_3$ ) gets smaller until  $\mu \approx 600 \text{ GeV}$  and it is not possible to find any region in the parameter space below this value ( $\mu \lesssim 600 \text{ GeV}$ ) for  $\tan \beta = 4$  (left panel), since this region is completely disallowed by the experimental bound [16]. On the other hand, as is shown in the right panel of Fig. 4, that the maximum value of the CP–odd percentage composition of  $h_3$  ( $\rho_3 \approx 0.0013\%$ ) occurs at  $|\mu| \approx 450 \text{ GeV}$  for  $\tan \beta = 30$ . As is in the left panel of Fig. 4, it again decreases with increasing  $|\mu|$ . Therefore (remembering  $M_A \propto |\mu|$  for the

model under concern) unless  $|\mu|$  is chosen smaller (equivalently unless the Peccei–Quinn scale is pushed down towards the lower limit of the allowed *axion window* [12, 15]) one cannot increase the CP–odd composition of the lightest Higgs boson.

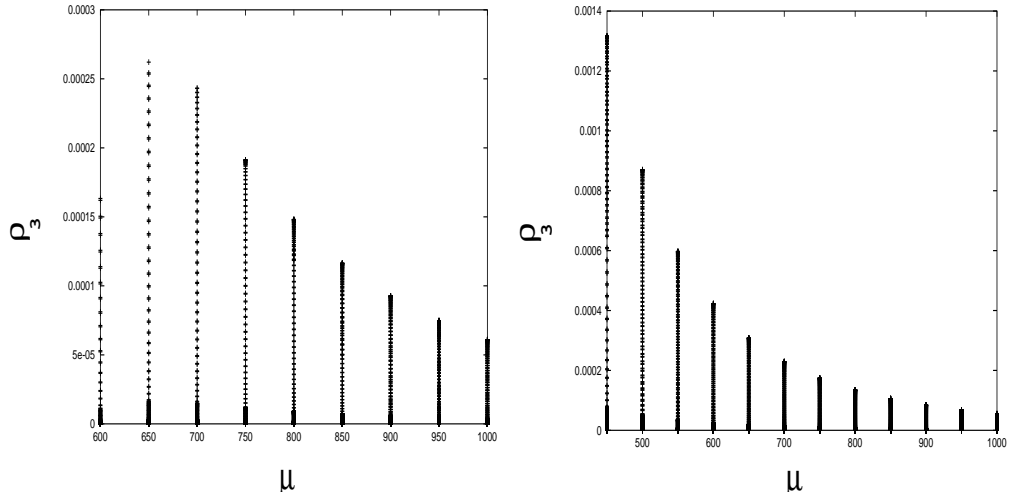


Figure 4: The CP–odd composition ( $\rho_3$ ) of the lightest Higgs ( $h_3$ ), as a function of  $\mu$  for  $\tan\beta = 4$  (left panel), and  $\tan\beta = 30$  (right panel).

One notes that, the lower limit on the lightest Higgs mass is directly correlated with its CP–odd composition, that is, as the lower bound on the lightest Higgs mass increases, its CP–odd composition decreases as will be indicated by Fig. 5

In Fig. 5, we show the variation of the lightest Higgs mass ( $m_{h_3}$ ) with its CP–odd composition ( $\rho_3$ ) for  $\tan\beta = 4$  (left panel),  $\tan\beta = 30$  (right panel), respectively. Both windows of the figure suggest that, lighter the Higgs boson, ( $m_{h_3}$ ), larger its CP odd composition ( $\rho_3$ ). From the left panel of Fig. 5, it is seen that the maximum value of the CP–odd composition of  $h_3$  starts from  $\approx 0.00027\%$  and decreases rapidly for  $\tan\beta = 4$  (left panel). On the other hand, as the right panel of the figure suggests that the maximum value of its CP–odd composition occurs at  $\rho_3 \approx 0.0013\%$  for  $\tan\beta = 30$ , and again relatively decreasing with the increasing mass, it reaches far below  $0.0002\%$  for  $m_{h_3} = 127\text{ GeV}$ .

One also notes that, the same kind of variation can be observed for all values of  $\tan\beta$ , ranging from 4 to 30. Therefore, one can conclude that possible increase in the lower experimental bound of the lightest Higgs mass

in future colliders will imply reduced CP-odd composition.

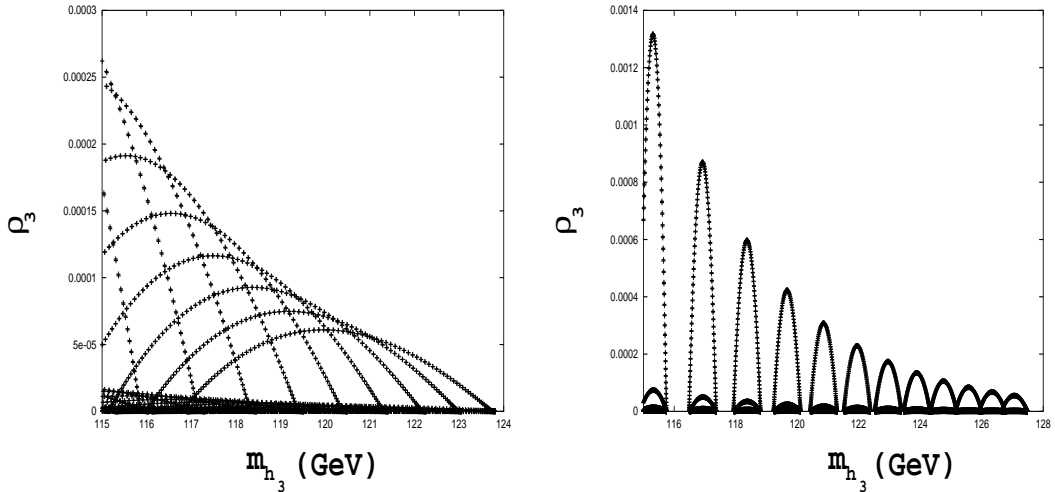


Figure 5: The variation of the mass ( $m_{h_3}$ ) of the lightest Higgs boson ( $h_3$ ), with its CP-odd composition ( $\rho_3$ ) for  $\tan \beta = 4$  (left panel) and  $\tan \beta = 30$  (right panel).

In the first part of our numerical analysis, we have studied the percentage CP compositions of the lightest Higgs boson  $h_3$ , in particular its CP-odd composition, as well as its mass for a given portion of the parameter space which are of prime importance in the light of present LEP experiments[16]. On the other hand, it is a well-known fact that the heavy Higgs bosons, which are out of reach of the present colliders, have no definite CP quantum numbers for most of the MSSM parameter space and it will be hard to observe them before NLC or TESLA operates. However, at this point, we also would like to discuss CP characteristics of the heavy Higgs bosons for the underlying model, in the low and high  $\tan \beta$  regimes, for completeness.

In Fig. 6, we show the variation of the mass of the second heavy scalar  $m_{h_2}$  with  $k_A$ , for all the values of  $\tan \beta$  ranging from 4 to 30. Since the two heavy scalars are degenerate in mass,  $k_A$  dependence of  $m_{h_2}$  is indicated in Fig. 5, for convenience. It is seen from the figure that the lower bound of  $m_{h_2}$  starts from 500 GeV, and extends to 5000 GeV, while  $M_A$  ranges from  $|\mu|$  to 5  $|\mu|$  for each  $\mu$  value. One notes that, for  $k_A = 1$  the masses of the heavy scalars changes from 500 GeV to 1000 GeV, lying right at the weak scale.

Depicted in Fig. 7, is the  $\varphi_{kt}$  dependence of  $\rho_1$ – $\rho_3$  designating the CP-even and CP-odd percentage compositions of the second scalar particle ( $h_2$ )

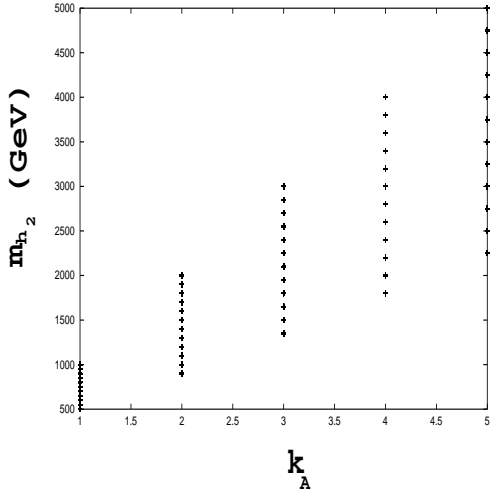


Figure 6: The mass of the second heavy scalar ( $m_{h_2}$ ) as a function of  $k_A$  for all values of  $\tan \beta$  changing from 4 to 30.

respectively, for  $\tan \beta = 4$  (left panel) and  $\tan \beta = 30$  (right panel). As is noticed from the figure that as the  $\rho_3$  component of  $h_2$  changes in between  $\approx 100\%$  and  $\approx 98.2\%$ , its  $\rho_1$  component becomes at most  $\approx 1.8\%$  for  $\tan \beta = 4$  (left panel). On the other hand, in passing to the large  $\tan \beta$  regime, one notes that there is a complementary behaviour of  $\rho_3$  (right panel). Starting from  $\varphi_{kt} = 0$  at the 100% level, it vanishes at  $\varphi_{kt} = \pi/2$  at the 0% level, then it increases to 100% at  $\varphi_{kt} = \pi$ , decreasing to 0% level again at  $\varphi_{kt} = 3\pi/2$ , it completes its behaviour at the 100% level. Its  $\rho_1$  component follows the same behaviour but it starts from  $\varphi_{kt} = 0$  at the 0% level. It is seen that though the CP-conserving points, namely  $\varphi_{kt} = 0, \pi, 2\pi$ , the particle under concern has a definite CP-parity. On the other hand, at the maximal CP-violation points, namely  $\varphi_{kt} = \pi/2, 3\pi/2$ , the CP-parity of the particle is completely reversed. And except for the points mentioned above, the particle has no definite CP characteristics. In summary,  $h_2$  is a pure pseudoscalar for small  $\tan \beta$  values, whereas its CP-parity swings significantly as the CP-phase varies in the large  $\tan \beta$  regime

As seen from Fig. 8,  $h_1$  has  $\approx 94\% \rho_1$  and  $\approx 1.8\% \rho_3$  composition for  $\tan \beta = 4$  (left panel) and the particle under concern is a CP-even scalar. In the large  $\tan \beta$  regime however, in accordance with the right panel of Fig. 7,  $h_1$  has no definite CP parity except for the pure CP-conserving and CP-violating points.

From the analyses of Figures 7 and 8, one can deduce that although the heavy scalar particles have definite CP parities for small  $\tan \beta$  values, they do not have definite CP characteristics for large  $\tan \beta$  and differ from the lightest Higgs boson in a sense that not only they have different masses but also they have indefinite CP characteristics.

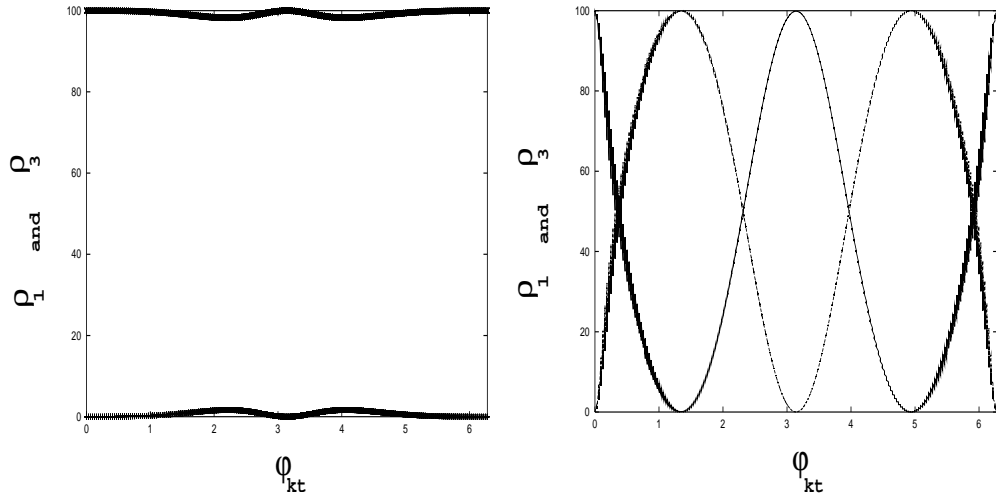


Figure 7:  $\rho_1$  (bottom curve) and  $\rho_3$  (top curve) components of  $h_2$  as a function of  $\varphi_{kt}$  for  $\tan \beta = 4$  (left panel) and  $\tan \beta = 30$  (right panel).

## 4 Conclusion

From the analyses of the masses and the CP compositions of the Higgs bosons, we conclude that:

- (i) The lightest Higgs mass is quite sensitive to the SUSY CP phases, thanks to which there arise new regions of the SUSY parameter space in which the present experimental constraints are satisfied,
- (ii) Although the percentage CP-odd composition of the lightest Higgs increases relatively with the increasing  $\tan \beta$ , it is still very small as compared to its CP-even compositions. The lower limit on the lightest Higgs mass is directly correlated with its CP-odd composition.
- (iii) The percentage CP-odd composition of the lightest Higgs (with a mass  $m_{h_3} \gtrsim 115 \text{ GeV}$ ) can not gain an appreciable value unless  $\mu$  is chosen smaller. For smaller values of  $\mu$ , however, the parameter space is constrained by the existing LEP bound on the lightest Higgs [16].

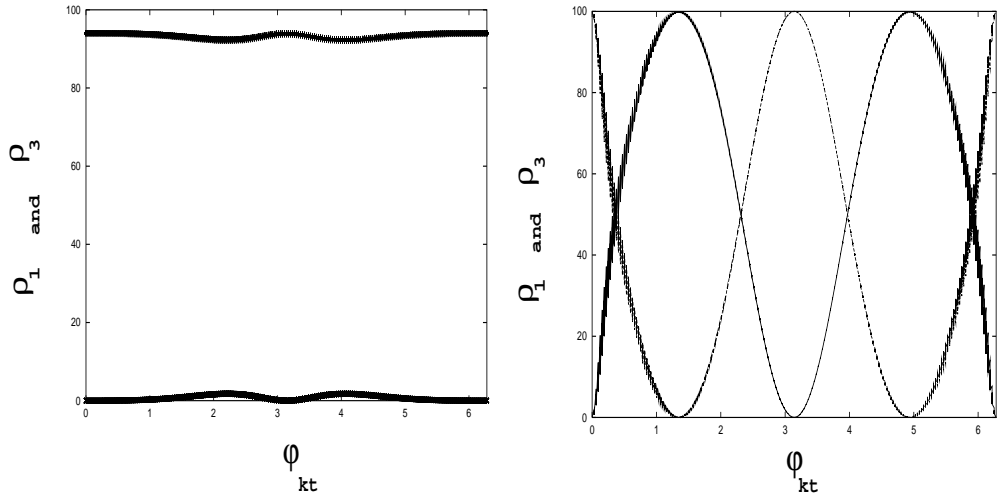


Figure 8:  $\rho_1$  (top curve) and  $\rho_3$  (bottom curve) components of  $h_1$  as a function of  $\varphi_{kt}$  for  $\tan \beta = 4$  (left panel) and  $\tan \beta = 30$  (right panel).

(iii) The remaining two heavy scalars have definite CP-parities in the small  $\tan \beta$  regime, but they have no definite CP-parities in the large  $\tan \beta$  regime. In this sense, they differ from the lightest Higgs as to their masses and their indefinite CP characteristics.

(iv) The gluino axion model, besides solving the strong CP and  $\mu$ -problems in an economical way, provides a quite restricted parameter space due to the naturalness requirements.

## 5 Acknowledgements

This work was partially supported by the Scientific and Technical Research Council of Turkey (TÜBİTAK) under the project, No:TBAG-2002(100T108).

## References

- [1] J. H. Christenson, J. W. Cronin, V. L. Fitch and R. Turlay, Phys. Rev. Lett. **13**, 138 (1964); . Alavi-Harati *et al.* [KTeV Collaboration], Phys. Rev. Lett. **83**, 917 (1999) [arXiv:hep-ex/9902029].
- [2] P. G. Harris *et al.*, Phys. Rev. Lett. **82**, 904 (1999).
- [3] C. G. Callan, R. F. Dashen and D. J. Gross, Phys. Lett. **B63**, 334 (1976); R. Jackiw and C. Rebbi, Phys. Rev. Lett. **37**, 172 (1976).
- [4] V. Baluni, Phys. Rev. **D19**, 2227 (1979); R. J. Crewther, P. Di Vecchia, G. Veneziano and E. Witten, Phys. Lett. **B88**, 123 (1979).
- [5] S. Dimopoulos and S. Thomas, Nucl. Phys. **B465**, 23 (1996) [arXiv:hep-ph/9510220].
- [6] D. A. Demir, Phys. Rev. D **62**, 075003 (2000) [arXiv:hep-ph/9911435].
- [7] M. Dugan, B. Grinstein and L. Hall, Nucl. Phys. **B255**, 413 (1985).
- [8] D. A. Demir, Phys. Lett. **B465**, 177 (1999) [arXiv:hep-ph/9809360]; Nucl. Phys. Proc. Suppl. **81**, 224 (2000) [arXiv:hep-ph/9907279].
- [9] A. Pilaftsis, Phys. Lett. **B435**, 88 (1998) [arXiv:hep-ph/9805373]; A. Pilaftsis, Phys. Rev. D **58**, 096010 (1998) [arXiv:hep-ph/9803297].
- [10] A. Pilaftsis and C. E. Wagner, Nucl. Phys. **B553**, 3 (1999) [arXiv:hep-ph/9902371].
- [11] D. A. Demir, Phys. Rev. **D60**, 055006 (1999) [arXiv:hep-ph/9901389].
- [12] D. A. Demir, E. Ma, Phys. Rev. **D62**, 111901 (2000) [arXiv:hep-ph/0004148].
- [13] D. A. Demir, E. Ma and U. Sarkar, J. Phys. G **G26**, L117 (2000) [arXiv:hep-ph/0005288]; D. A. Demir and E. Ma, J. Phys. G **27**, L87 (2001) [arXiv:hep-ph/0101185].
- [14] R. D. Peccei and H. R. Quinn, Phys. Rev. Lett. **38**, 1440 (1977).

- [15] J. E. Kim, Phys. Rev. Lett. **43**, 103 (1979); M. A. Shifman, A. I. Vainshtein and V. I. Zakharov, Nucl. Phys. **B166**, 493 (1980); M. Dine, W. Fischler and M. Srednicki, Phys. Lett. **B104**, 199 (1981).
- [16] LEPC, Nov 3, 2000, P Igo-Kemenes  
<http://www.cern.ch/LEPHIGGS/talks/index.html>.  
 Questions and Answers .. following the LEPC, Nov 6, 2000  
<http://www.cern.ch/LEPHIGGS/papers/index.html>.
- [17] J. R. Espinosa and R. Zhang, JHEP **0003**, 026 (2000) [arXiv:hep-ph/9912236]. M. Carena, H. E. Haber, S. Heinemeyer, W. Hollik, C. E. Wagner and G. Weiglein, Nucl. Phys. B **580**, 29 (2000) [arXiv:hep-ph/0001002].
- [18] H. E. Haber and R. Hempfling, Phys. Rev. Lett. **66**, 1815 (1991).
- [19] Y. Okada, M. Yamaguchi and T. Yanagida, Prog. Theor. Phys. **85**, 1 (1991); J. Ellis, G. Ridolfi and F. Zwirner, Phys. Lett. B **257**, 83 (1991); J. Ellis, G. Ridolfi and F. Zwirner, Phys. Lett. B **262**, 477 (1991);
- [20] R. Hempfling and A. H. Hoang, Phys. Lett. B **331**, 99 (1994) [arXiv:hep-ph/9401219].
- [21] P. H. Chankowski, S. Pokorski and J. Rosiek, Nucl. Phys. B **423**, 497 (1994).
- [22] Y. Okada, M. Yamaguchi and T. Yanagida, Phys. Lett. B **262**, 54 (1991); K. Sasaki, M. Carena and C. E. Wagner, Nucl. Phys. B **381**, 66 (1992); H. E. Haber and R. Hempfling, Phys. Rev. D **48**, 4280 (1993) [arXiv:hep-ph/9307201].
- [23] J. A. Casas, J. R. Espinosa, M. Quiros and A. Riotto, Nucl. Phys. B **436**, 3 (1995) [Erratum-ibid. B **439**, 466 (1995)] [arXiv:hep-ph/9407389]; M. Carena, M. Quiros and C. E. Wagner, Nucl. Phys. B **461**, 407 (1996) [arXiv:hep-ph/9508343]; M. Carena, J. R. Espinosa, M. Quiros and C. E. Wagner, Phys. Lett. B **355**, 209 (1995) [arXiv:hep-ph/9504316]; H. E. Haber, R. Hempfling and A. H. Hoang, Z. Phys. C **75**, 539 (1997) [arXiv:hep-ph/9609331].

- [24] S. Heinemeyer, W. Hollik and G. Weiglein, Phys. Lett. B **440**, 296 (1998) [arXiv:hep-ph/9807423].
- [25] T. Ibrahim and P. Nath, Phys. Rev. D **63**, 035009 (2001) [arXiv:hep-ph/0008237].
- [26] S. Y. Choi, M. Drees and J. S. Lee, Phys. Lett. **B481**, 57 (2000) [arXiv:hep-ph/0002287];
- [27] M. Carena, J. Ellis, A. Pilaftsis and C. E. Wagner, Nucl. Phys. **B586** 92 (2000) [arXiv:hep-ph/0003180].
- [28] D. A. Demir, Phys. Rev. **D60**, 095007 (1999) [arXiv:hep-ph/9905571]; S. Y. Choi, arXiv:hep-ph/9908397.
- [29] S. Y. Choi and J. S. Lee, Phys. Rev. D **61**, 015003 (2000) [arXiv:hep-ph/9907496]; Phys. Rev. D **61**, 111702 (2000) [arXiv:hep-ph/9909315]; Phys. Rev. D **61**, 115002 (2000) [arXiv:hep-ph/9910557]; Phys. Rev. D **62**, 036005 (2000) [arXiv:hep-ph/9912330].